Hindawi
International Journal of Digital Multimedia Broadcasting
Volume 2020, Article ID 9578521, 11 pages
https://doi.org/10.1155/2020/9578521

Research Article

Capacity Improvement for DVB-NGH with Dual-Polarized MIMO Spatial Multiplexing and Hybrid Beamforming

Huu Trung Nguyen,[1] **Trung Tan Le**,[1] **and Trung Hien Nguyen**[2]

[1]*School of Electronics and Telecommunications, Hanoi University of Science and Technology, Hanoi 10000, Vietnam*
[2]*Department of Electronics and Telecommunications, Posts and Telecommunications Institute of Technology, Hanoi 10000, Vietnam*

Correspondence should be addressed to Huu Trung Nguyen; trung.nguyenhuu@hust.edu.vn

Received 2 September 2019; Revised 13 July 2020; Accepted 27 July 2020; Published 17 August 2020

Academic Editor: Quoc-Tuan Vien

Multiple-input multiple-output (MIMO) antenna scheme is an effective technique for future terrestrial broadcasting systems such as digital video broadcasting-next-generation handheld (DVB-NGH) to overcome the limits on information theory of traditional single-antenna wireless communications without any additional bandwidth or increased transmit power. In this paper, we propose a hybrid beamforming scheme for dual-polarized MIMO spatial multiplexing DVB-NGH broadcasting systems. The system of interest makes use of phase shifters and amplitude attenuators for the digital-analog precoder at beamforming stage of the transmitter end to maximize the signal-to-noise ratio to increase the channel capacity of the DVB-NGH systems. At the receiver end, the maximum likelihood (ML) detector is used to evaluate the system performance. We consider the signal-to-interference-and-noise ratio (SINR) and the achievable average capacity for the DVB-NGH MIMO with various FFT sizes, number of transmit antennas, and different modulation schemes. The performance results on bit error rate, channel capacity, and beampatterns show that the proposed hybrid beamforming and dual-polarized MIMO spatial multiplexing schemes provide more robustness against signal interference by beamforming and/or nulling techniques. The simulation results also show that the proposed system achieves higher capacity than the existing MIMO schemes for the DVB-NGH systems.

1. Introduction

Digital video broadcasting (DVB) is a family of standardized technologies developed for TV broadcasting over terrestrial, cable, satellite, and mobile communication systems [1]. In the last decade, DVB is an area of intensive development and standardization activities such as DVB-H (Handheld), Media FLO (Forward Link Only), and DVB-SH (Satellite to Handheld) [2–4]. They are developed to support large-scale consumption of mass multimedia services such as mobile television (TV). However, mobile TV services did not fulfill the initial expectations due to the lack of a successful business model and the high costs associated to the development of new mobile broadcasting networks. Today, a new generation of mobile broadcasting technologies is emerging due to the continuously increasing requirements and expectations of both users and operators that incorporate the latest advances in wireless communications which provide significant capacity and coverage improvements. To date, the latest emerging member of DVB family standards is DVB-NGH (next-generation handheld) [5]. It is the mobile evolution of the second-generation digital terrestrial TV broadcasting technology based on the physical layer of DVB-T2, the most advanced digital terrestrial TV (DTT) technology in the world [6]. Therefore, it can be incorporated in DVB-T2 transmissions, allowing the reuse of spectrum and infrastructure of DVB-T2, offering more robustness, flexibility, and at least 50% more spectrum efficiency than any other technology [7].

DVB-NGH was created with the objectives of increasing the coverage performance area and network capacity not only outperforming the previous existing mobile broadcasting standards DVB-H and DVB-SH but also optimizing DVB-T2 in many aspects [5]. DVB-NGH is of significant interest among the wireless operators, since it allows the transmission of IP (Internet Protocol) mass multimedia content to a wide range of mobile devices, from wearable devices

such as earphones, mobile phones, and MP3 players to laptops and vehicle-mounted receivers at very high data rates [8]. Compared to DVB-T2, DVB-NGH uses Scalable Video Coding (SVC) technology with Multiple Physical Layer Pipes (MPLPs) for graceful service degradation, TFS (Time-Frequency Slicing) technique that enables multiple frequency channels to be combined into a single wider channel in order to improve the efficiency and robustness of digital television terrestrial (DTT) transmissions [9, 10]. In streaming service data, DVB-NGH uses RoHC (Robust Header Compression) method to reduce the overhead due to IP encapsulation, additional satellite component for increased coverage area, improved signaling robustness [5]. DVB-NGH allows efficient transmission of local services within enhanced Single-Frequency Network (eSFN) [11]. DVB-NGH improves SFN planning flexibility in the 4K mode [12]. Finally, DVB-NGH is the first broadcasting system to incorporate multiple-input multiple-output (MIMO) antenna schemes as the key technology not only to improve the robustness of the transmitted signal by exploiting the spatial diversity of the MIMO channel but also to achieve increased data rates through spatial multiplexing. Recently, reciprocity calibration for massive MIMO has been studied for future terrestrial broadcasting technologies [13]. In this work, Luo et al. proposed a novel and innovative closed-loop reciprocity calibration method for massive MIMO systems with a better performance compared to the existing methods. A lab measurement setup is built for BS hardware impairments' measurement and the implementation.

1.1. Related Works. Nowadays, MIMO is a key technology to increase the capacity and system reliability without any additional wireless bandwidth for terrestrial broadcasting system [14–16]. Dai et al. addressed in [14] the key technologies and research trends for next-generation digital television terrestrial broadcasting systems, including the discussion about status, technical challenges, and more importantly the future research trends. In addition, MIMO technology, OFDM-based transmission, modulation, and channel coding were focused as the common technologies to increase the system capacity and improve the transmission reliability. The authors in [15–17] described the benefits of MIMO that motivated its incorporation in DVB-NGH. In these works, the structure of MIMO channel precoders for digital terrestrial TV systems and enhanced spatial multiplexing phase hopping (eSM-PH) as well as the required elements at the transmitter and receiver terminals to decode the MIMO eSM-PH 2×2 transmission was presented against the unprecoded 4×2 MIMO scheme. Performance of practical MIMO systems and compared to SISO using DVB-NGH physical layer has been assessed for the 2×2 MIMO scheme with spatial multiplexing to support four transmit antennas; MIMO could provide significant carrier to noise ratio (CNR) reductions [15]. The system capacity in bpc vs. the CNR required to achieve the selected QoS criterion for eSM-PH with different deliberated transmitted power over correlated Rice fading channel was clearly provided. Moreover, MIMO rate-2 codes allowed to increase data rates through spatial multiplexing. DVB-NGH MIMO rate-2 schemes were the best option suited for outdoor medium/high signal use cases such as tablet PCs and automotive reception as the generally lower signal-to-noise ratios (SNR) of portable/indoor reception substantially reduce the available multiplexing gain that may be exploited [16]. However, in the DVB-NGH physical layer architecture perspective, these studies did not consider the MIMO beamforming design on the performance of the MIMO channel precoder.

Traditional MIMO-beamforming systems require a dedicated radio frequency (RF) chain for each antenna element, which becomes impractical with massive MIMO systems due to either cost or power consumption. To reduce the number of RF chains, hybrid beamforming (HBF), which combines RF analog and baseband digital beamformers, has been proposed as a promising solution to enhance the network capacity and coverage of next-generation mobile wireless communication [18–20]. Sohrabi and Yu presented in [18, 19] the transceiver design for maximizing the spectral efficiency of a large-scale MIMO system with hybrid beamforming architecture where the number of RF chains is equal to the number of data streams. The hybrid beamforming structure can achieve the same performance as the fully digital beamforming scheme if the number of RF chains at each end is greater than twice the number of data streams. The design could achieve a rate close to that of optimal exhaustive search and use the extra RF chains to significantly improve the system performance in the case of low-resolution phase shifters (PSs).

Moreover, millimeter wave (mmWave) cellular systems will enable gigabit-per-second data rates thanks to the large bandwidth available at mmWave frequencies. Due to the high cost and power consumption of gigasample mixed-signal devices, mmWave precoding will likely be divided among the analog and digital domains. The large number of antennas and the presence of analog beamforming require the development of mmWave-specific channel estimation and precoding algorithms [20–24]. A hybrid analog/digital precoding algorithm that overcomes the hardware constrains on the analog-only beamforming, approaching the performance of digital solutions, was proposed in [20]. In [21], the problem of mmWave precoder design as a sparsity-constrained signal recovery was formulated using orthogonal matching pursuit. This framework could be applied to the problem of designing practical MMSE combiners for mmWave systems. Most recently, Magueta et al. proposed a hybrid multiuser equalizer for the uplink of broadband mmWave systems with dynamic subarray antennas [22]. The hybrid subconnected architectures were designed for the number of required PSs which was lower than in fully connected architectures with a set of only analog precoded users transmitting to a base station and sharing the same radio resources. At the receiver end, the hybrid multiuser equalizer was designed by minimizing the sum of the mean square error (MSE) of all subcarriers, considering the digital part is iteratively computed as a function of the analog part and the analog equalizer with dynamic antenna mapping that was derived to connect the best set of antennas to each RF chain. This designed hybrid dynamic two-step equalizer achieved the performance close to the fully connected

counterpart, although it is less complex in terms of hardware and signal processing requirements. In addition, the same authors in [23] proposed the iterative analog-digital multiuser equalizer by minimizing the sum of the MSE of the data estimates over the subcarriers assuming that the analog part was fixed for all subcarriers while the digital part computed on a per subcarrier basis. The bit error rate (BER) of the hybrid system was derived and compared with other hybrid equalizer schemes, which were recently designed for mmWave MIMO systems. This technique showed that the performance of the developed analog-digital multiuser equalizer was close to the full-digital counterpart and outperforms the previous hybrid approach. In [24], Hefnawi recently proposed a hybrid beamforming scheme for mmWave heterogeneous networks formed with one macrocell base station (BS) and multiple small-cell BS equipped with large-scale antenna arrays that employ hybrid analog and digital beamforming. Digital beamforming weights were optimized to maximize the received signal-to-interference-plus-noise ratio (SINR) of the effective channels. In this study, the beampatterns and the ergodic channel capacity were evaluated with only four RF chains while requiring considerably less computation complexity. To our knowledge, the hybrid beamforming schemes using analog-digital beamforming and dual-polarized MIMO spatial multiplexing for the DVB-NGH system have yet to be addressed in the literature.

In this paper, we therefore present a comprehensive study on the performance of the analog-digital beamforming using dual-polarized MIMO spatial multiplexing for the DVB-NGH systems. Unlike previous works, the objective of this architecture is to improve capacity as well as the robustness of the received signal. MIMO technique is employed to improve coverage area and increase the channel capacity of the DVB-NGH systems. Therefore, the hybrid beamforming scheme that combines with dual-polarized MIMO spatial multiplexing is supposed to meet the expectation for the future broadcasting systems such as DVB-NGH.

1.2. Main Contributions. In this paper, we propose a solution on the category of performance-oriented technologies to develop DVB-NGH systems which includes OFDM-based transmission, modulation schemes, and channel coding and especially employing the MIMO technology. Therefore, our design options include the following:

(i) We design and analyze the performance on bit error rate and ergodic channel capacity of the hybrid beamforming dual-polarized MIMO spatial multiplexing with the eSM-PH structure. The proposed architecture interest makes use of phase shifters and amplitude attenuators for the digital-analog precoder at beamforming stage to maximize the signal-to-noise ratio to increase the capacity of the DVB-NGH systems

(ii) The dual-polarized MIMO analog precoder is designed at both the transmitter and receiver sides. In addition, the maximum likelihood (ML) detector is used at the hybrid receiver to evaluate the system performance purposes. For the case studies, we clearly describe the signal-to-interference-and-noise ratio (SINR) and the corresponding achievable average capacity for the DVB-NGH MIMO with various FFT sizes, number of transmit antennas, and different modulation schemes

Table 1: Notation adopted in the paper.

Operator	Description
$\mathrm{tr}(\bullet)$	Trace of a matrix
$(\bullet)^*$	Conjugate of a matrix
$(\bullet)^T$	Transpose of a matrix
$(\bullet)^H$	Hermitian of a matrix
$\mathrm{diag}(\mathbf{a})$	Diagonal matrix where the diagonal entries are equal to vector $\mathbf{a}$
$\mathbf{A}$	Represents the elements of the n-th row and m-th column of a matrix
$\mathbf{a}$	Represents a vector
a	Represents a scalar
$\mathbb{E}_{\mathbf{H}}[\bullet]$	Expectation
$\|\|\mathbf{A}\|\|_F$	The Frobenius norm of $\mathbf{A}$
$\mathrm{tr}(\mathbf{A})$	The trace of the matrix $\mathbf{A}$
$\mathbf{I}_{N_m}$	Identity matrix $N \times N$

The remainder of this paper is organized as follows. Section 2 describes the system model description adopted in the work. Section 3 describes a MIMO rate-2 case study. In Section 4, we show the main performance results and discussions on bit error rate, ergodic capacity, and beampattern of the proposed scheme. Finally, the conclusions and directions are presented in Section 5.

1.3. Notations. Capital boldface letters denote matrices, and lower boldface letters denote column vectors. The remaining notations in this paper are presented in Table 1.

2. System Model Description

In this section, we describe the hybrid beamforming scheme for improving the performance of dual-polarized MIMO spatial multiplexing DVB-NGH broadcasting systems.

The block diagram of the proposed dual-polarized MIMO spatial multiplexing combining with the digital-analog beamforming for DVB-NGH system is illustrated in Figure 1. We consider the system with K data streams may be simultaneously transmitted in the same bandwidth using $N_T = K$ transmitter antennas. The transmitted signal then being separated into K respective data streams by way of a set of $N_R = K \times M$ antennas deployed at the receiver. In the system model, we use partially connected structure for hybrid beamforming, where each RF chain is connected to an array of M dual-polarized antennas. Such a structure has a lower hardware complexity compared to fully connected, but beamforming gain is reduced [25].

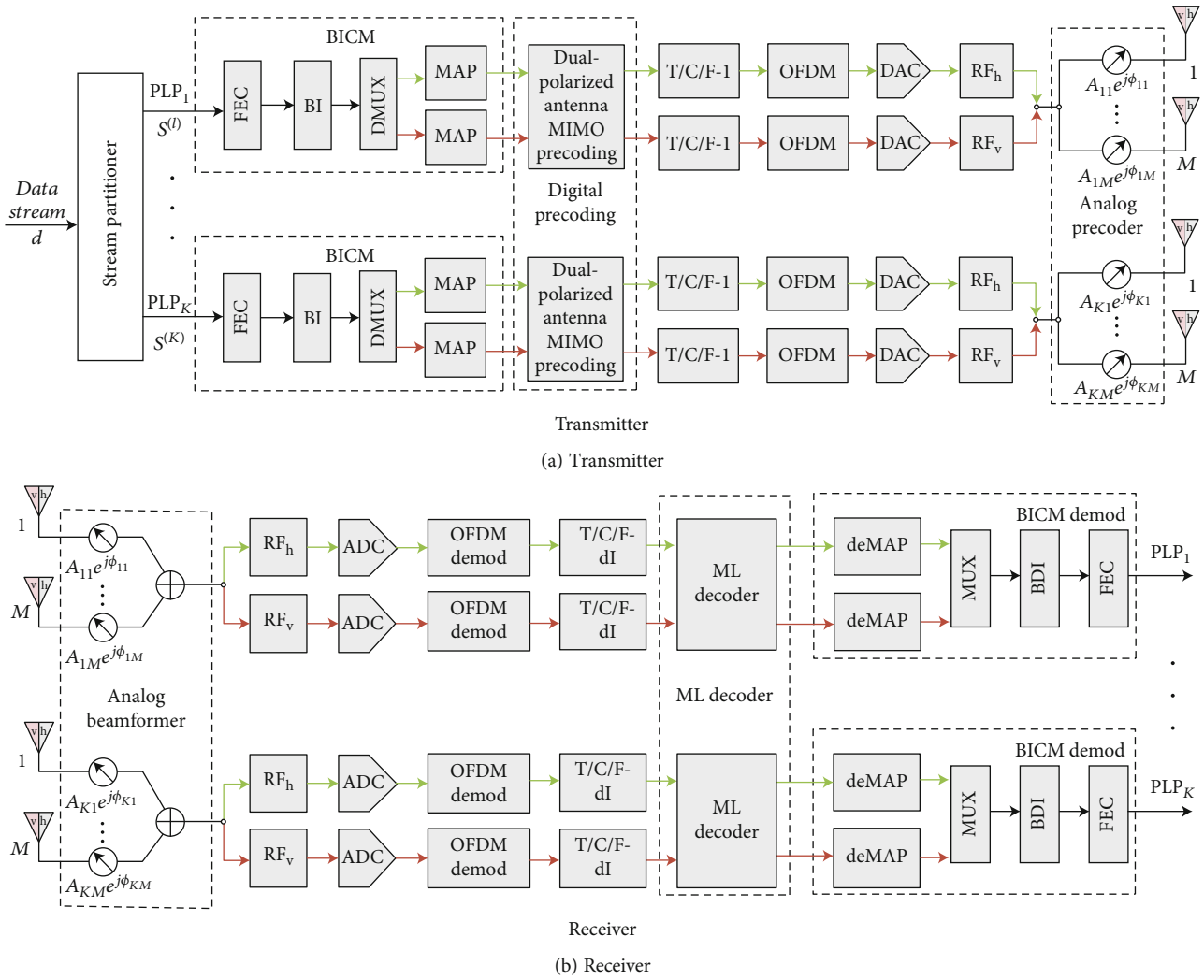

Figure 1: Block diagram of a hybrid digital-analog beamforming MIMO DVB-NGH system: (a) transmitter side; (b) receiver side.

At the transmitter side (Figure 1(a)), the Bit-Interleaved Coded Modulation (BICM) module is one of the most important modules as it provides the error correction capability for the system. The input to the BICM module consists of one or more logical data streams which are separated from services data stream d by a stream partitioner. Each logical data stream is carried by one Physical Layer Pipe (PLP) and associated with a modulation constellation, a forward-error correcting (FEC) protection mode, and a time interleaving depth [26]. The structure of DVB-NGH BICM module consists of serial concatenation of a FEC encoding subsystem which performs outer coding using Bose-Chaudhuri-Hocquenghem (BCH) codes, inner coding using a low-density parity-check code (LDPC), bit interleaving (BI), and a constellation mapper (MAP) [27].

2.1. Design of Dual-Polarized MIMO Digital Precoder. Figure 2 illustrates the dual-polarized MIMO precoder as a digital precoder for each data stream input. The precoder is designed based on spatial multiplexing (SM) to increase the channel spectral efficiency by providing reliable performance over erasure channel [28]. The digital precoder consists of three different steps of linear precoding, phase hopping, and power calibration. In the first step, the transmitted symbol is performed by the linear precoding to correlate the transmitted signal on different transmitting antennas. Therefore, even if one or more channel links encounter erasure phenomenon, the transmitted signal can still be recovered from the other link signals [29]. For each PLP k ($k = 1 \cdots K$), the precoded data symbol can be expressed as

$$\mathbf{x}^{(k)} = \mathbf{\Theta}\mathbf{s}^{(k)}, \tag{1}$$

where the precoding matrix is determined by

$$\mathbf{\Theta} = \begin{bmatrix} \cos\theta & -\sin\theta \\ \sin\theta & \cos\theta \end{bmatrix}. \tag{2}$$

In equation (2), if the rotation phase $\theta = 33.3^\circ$ and $\theta = 45^\circ$, we have eSM (enhanced SM) and Hadamard SM (hSM), respectively. The rotation phase θ has very little impact on the system's performance [16]. The phase hopping eSM (PH-eSM) consists of a phase rotation to the

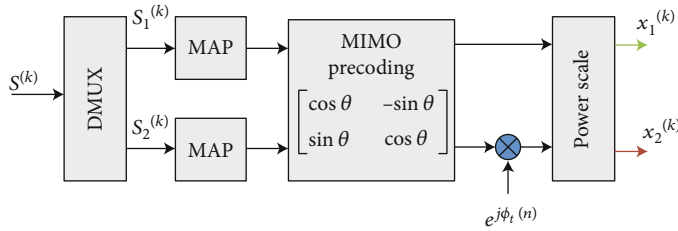

Figure 2: Dual-polarized antenna MIMO precoder.

symbols of the second transmitting antenna by the multiplication with the term $e^{j\varphi_t(n)}$. The precoded data symbol with phase hopping is therefore expressed as

$$\mathbf{x}^{(k)} = \mathbf{\Psi\Theta s}^{(k)}, \tag{3}$$

where the $\mathbf{\Psi}$ is given by

$$\mathbf{\Psi} = \begin{bmatrix} 1 & 0 \\ 0 & e^{j\varphi_t(n)} \end{bmatrix}. \tag{4}$$

In equation (4), $\varphi_t(n) = (2\pi/N)n, n = 0, \cdots, (N_{\text{cell}}/2) - 1$, and $N = 9$ is the hopping period and N_{cell} is the number of cells per FEC codeword. The phase hopping periodically changes the phase of symbols transmitted by one of two antennas within one FEC block. This is performed by the multiplication with the term of $e^{j\varphi_t(n)}$. The phase rotation is initialized to 0° at the beginning of each FEC block and is incremented by $2\pi/9$ for every cell pair. This hopping phase enhances circularly the robustness against the transmitting antenna orientation to increase the diversity [30].

The ST coded data symbols with unequal power can be written as

$$\mathbf{x}^{(k)} = \mathbf{\Psi\Theta P s}^{(k)}, \tag{5}$$

where $\mathbf{P}$ is defined as a matrix to scale the power between two antennas. It can be expressed as

$$\mathbf{P} = \begin{bmatrix} \sqrt{\rho} & 0 \\ 0 & \sqrt{1-\rho} \end{bmatrix}. \tag{6}$$

For instance, when QPSK and 16-QAM are applied to the two antennas, ρ is set to 1/3. This means twice power is allocated to 16-QAM than the QPSK symbols. It is to increase the robustness of the higher order constellation under the constraint of the total signal power.

The combination of eSM and the phase hopping is the so-called eSM-PH. The MIMO rate-2 code of the DVB-NGH system is expressed as

$$\begin{bmatrix} x_1^{(k)} \\ x_2^{(k)} \end{bmatrix} = \begin{bmatrix} 1 & 0 \\ 0 & e^{j\varphi_t(n)} \end{bmatrix} \begin{bmatrix} \cos\theta & -\sin\theta \\ \sin\theta & \cos\theta \end{bmatrix} \begin{bmatrix} \sqrt{\rho} & 0 \\ 0 & \sqrt{1-\rho} \end{bmatrix} \begin{bmatrix} s_1^{(k)} \\ s_2^{(k)} \end{bmatrix}. \tag{7}$$

The digital precoder for the overall DVB-NGH system is represented as $\mathbf{D} = \text{diag}[\bar{\mathbf{d}}_1, \bar{\mathbf{d}}_2, \cdots \bar{\mathbf{d}}_K]$, where $\bar{\mathbf{d}} = \mathbf{\Psi\Theta P} \in \mathbb{C}^{2\times 2}$. K data symbols are precoded by $\mathbf{D}$; each symbol $\mathbf{x}^{(k)}$ is then passed through the k-th RF chain.

The digital domain signal from one RF chain is then fed to M transmitting antennas to perform transmit analog precoding. The analog precoder vector is expressed as

$$\bar{\mathbf{a}}_k = [a_{k1}, a_{k2}, \cdots a_{kM}]^T \in \mathbb{C}^{M\times 1}, \tag{8}$$

where $a_{ij} = A_{ij}e^{j\phi_{ij}}$, A_{ij} is the amplitude factor and ϕ_{ij} is the phase shift. Finally, every data symbol is transmitted by the subantenna array of M antennas.

2.2. Receivers. Consider the receiver side, where the hybrid analog-digital beamforming architecture is shown in Figure 1(b). The received signal for all K data symbols $\mathbf{r} = [r_1, r_2, \cdots r_K]^T$ is expressed as

$$\mathbf{r} = \sqrt{\text{SNR}}\mathbf{HADx} + \mathbf{n} = \sqrt{\text{SNR}}\mathbf{HGx} + \mathbf{n}, \tag{9}$$

where $\bar{\mathbf{h}}_k = [h_{11}, h_{12}, \cdots, h_{kM}] \in \mathbb{C}^{1\times M}$, $\mathbf{h}_k = [\mathbf{0}_{1\times M(k-1)}, \bar{\mathbf{h}}_k, \mathbf{0}_{1\times M(K-k)}] \in \mathbb{C}^{1\times KM}$, and $\mathbf{H} = [\mathbf{h}_1, \mathbf{h}_2, \cdots, \mathbf{h}_K] \in \mathbb{C}^{K\times KM}$ that is given by

$$\mathbf{H} = \begin{bmatrix} \bar{\boldsymbol{h}}_1 & 0 & \cdots & 0 \\ 0 & \bar{\boldsymbol{h}}_2 & \vdots & 0 \\ \vdots & \vdots & \ddots & \\ 0 & 0 & \cdots & \bar{\boldsymbol{h}}_K \end{bmatrix} = \begin{bmatrix} h_{11} & h_{12} & \cdots & h_{1M} & & & 0 \\ & & & & \ddots & & \\ & & & & & \ddots & \\ 0 & & & & & & h_{K1} & h_{K2} & \cdots & h_{KM} \end{bmatrix}. \tag{10}$$

The analog precoder $\mathbf{A}$ of the receiver is represented in the following matrix form:

$$\mathbf{A} = \begin{bmatrix} \bar{\mathbf{a}}_1 & \mathbf{0} & \cdots & \mathbf{0} \\ \mathbf{0} & \bar{\mathbf{a}}_2 & \vdots & \mathbf{0} \\ \vdots & \vdots & \ddots & \vdots \\ \mathbf{0} & \mathbf{0} & \vdots & \bar{\mathbf{a}}_K \end{bmatrix}. \tag{11}$$

In this expression, the analog precoder vector of receiver, $\bar{\mathbf{a}}_i$, is defined similarly to those of the transmitter. K data symbols are represented as $\mathbf{x} = [x_1, x_2, \cdots, x_K]^T$. Moreover, in equation (9), the total noise of $\mathbf{n} = [n_1, n_2, \cdots, n_K]^T$, where n_k is the complex Gaussian random variable with zero means

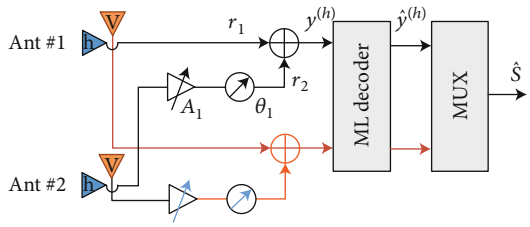

Figure 3: The DVB-NGH MIMO rate-2 receiver diagram.

Table 2: Study cases.

Case	Study cases
1	BER for the MIMO rate-2 mode, FFT 8 K/16 K, 64- or 256-QAM constellation modulation schemes
2	Capacity for the MIMO rate-2 mode and $N_s = 4$, 16 K FFT mode, 64-QAM

and a variance of σ^2, and $\mathbf{G} = \mathbf{AD}$ represents the joint hybrid precoding matrix with the size of $KM \times K$.

2.3. Capacity Analysis. Recall the ergodic capacity of MIMO channel assuming perfect channel knowledge at both transmitter and receiver with zero-mean Gaussian distribution inputs. The ergodic capacity can be expressed in general form as [31]

$$C_H = \mathbb{E}_{\mathbf{H}}\left[\max_{\mathbf{Q}:\mathrm{Tr}(\mathbf{Q})=P} \log_2\left|\mathbf{I}_{N_m} + \mathrm{SNR}\mathbf{HQH}^H\right|\right], \quad (12)$$

where the covariance of the input data $\mathbf{Q}$ is written as

$$\mathbf{Q} = \mathbf{GG}^H. \quad (13)$$

Therefore, equation (12) is given by

$$C_H = N_m \log_2\left(\det\left(\mathbf{I}_{N_m} + \mathrm{SNR}\mathbf{HQ}_X\mathbf{H}^H\right)\right), \quad (14)$$

where $\mathbf{I}_{N_m}$ denotes the identity matrix of dimensions $N_m \times N_m$, $\mathbf{Q}_X = (1/N_m)\mathbf{I}_{N_m}$, and $\mathbf{H}^H$ is the complex conjugate transpose of $\mathbf{H}$, $N_m = \min(N_T, N_R)$. When the channel matrix is square and orthogonal ($\mathbf{HH}^H = \mathbf{I}$), then with an identically distributed data input channel capacity can be rewritten as [32]

$$C_H = \mathrm{N}_m \log_2\left(1 + \frac{\mathrm{SNR}}{N_m}\right). \quad (15)$$

The capacity is linearly scaled with the number of transmitter antennas for an increasing SNR. In general, it can be demonstrated that an orthogonal channel as the one used in the previous example maximizes the capacity in MIMO systems. In an identically distributed channel with flat fading, the channel matrix becomes almost orthogonal when the number of transmitter antennas is high [33]. When the number of transmitter and receiver antennas is different, the capacity increase is limited to the minimum number of them. The purpose of analog beamforming is to raise the SNR. In the next section, we consider a MIMO rate-2 case and estimate the SNR for capacity evaluation.

Table 3: Simulation parameters.

Parameter	Value
PLP	2, 4
Number of substreams in Demux	2
Number of transmitter antennas	1, 2, 4, 8
Number of RF chains	2, 4
Number of receiver antennas	2, 4
Bandwidth	8 MHz
Modulation	64-QAM and 256-QAM
Carriers (FFT size)	8 K, 16 K
Constellation rotation	2D ($b = 0.2890$ 16-QAM, $b = 0.1495$ 64-QAM)
Interleavers	B-C-T-FI
FEC encoding and code rate	16 K LDPC code 8/15
Guard interval	1/16
PAPR reduction	Active constellation extension (ACE)

3. MIMO Rate-2 Case Study

In this section, we describe the MIMO spatial multiplexing that is specified in DVB-NGH as MIMO rate-2 codes. The term "rate-2" basically stands for the transmission of two independent streams. MIMO rate-2 codes in DVB-NGH use cross-polar antenna arrangement (antennas with orthogonal polarization) with two transmitter antennas and two receiver antennas (the 2×2 MIMO system).

The DVB-NGH MIMO rate-2 receiver diagram is illustrated in Figure 3. In this scheme, we clarify the amplitude factor of A_i and the phase factor of ϕ_i. Considering the horizontally polarized part of the system, the received signal can be written as

$$\begin{aligned} r_1 &= h_1 x + n_1, \\ r_2 &= A_1 e^{j\phi_1} h_2 x + A_1 e^{j\phi_1} n_2, \\ y^{(h)} &= r_1 + r_2 = x\left(h_1 + A_1 e^{j\phi_1} h_2\right) + n_1 + A_1 e^{j\phi_1} n_2, \end{aligned} \quad (16)$$

where superscript h denotes the polarized antenna horizontally, r_1 and r_2 represent the received signal at the first receiver antenna and the received signal at the second receiver antenna, respectively. x, n_1, and n_2 are the transmitted signal, the noise component at the first receiver antenna, and the parameter representing noise component at the second receiver antenna, respectively. θ_1 and A_1 are the phase factor between the received signal at the first and second receiver antennas and the amplitude factor, respectively.

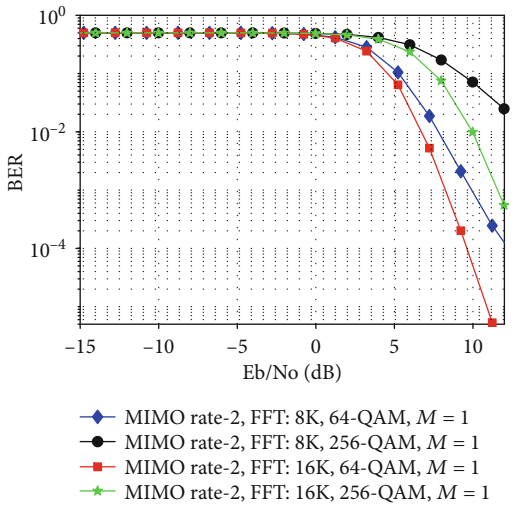

(a) BER vs. Eb/No for various modulation schemes, the transmitter antennas of $M = 1$

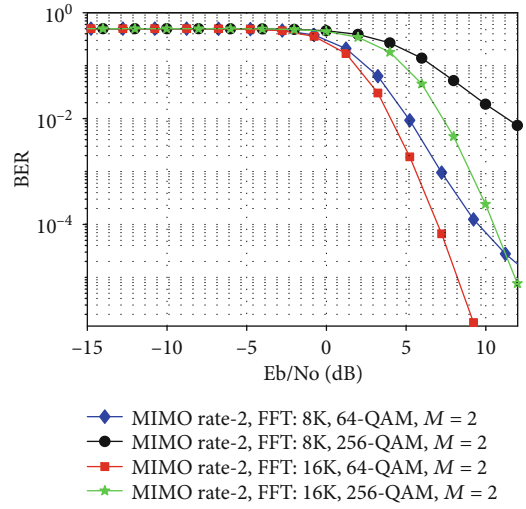

(b) BER vs. Eb/No for various modulation schemes and the FFT size, the transmitter antennas of $M = 2$

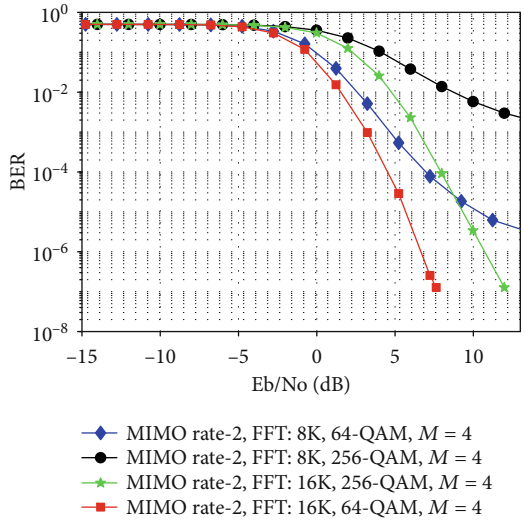

(c) BER vs. Eb/No for various modulation schemes, the transmitter antennas of $M = 4$

FIGURE 4: The BER performance against Eb/No for MIMO rate-2 using the modulation schemes of 64-QAM and 256-QAM with the FFT size of 8 K and 16 K for various numbers of antenna element M at the analog precoder.

When the DVB-NGH MIMO system uses N transmitter and M receiver antennas, the received signal at the receiver side can be represented as

$$r_k = \sum_{i=1}^{N} \left(A_{k-1} e^{j\phi_{k-1}} h_{ik} x + A_{k-1} e^{j\phi_{k-1}} n_k \right), \tag{17}$$

and the output of the analog beamformer is expressed as

$$y_k = \sum_{i=1}^{M} r_k, \tag{18}$$

where $A_0 = 1$ and $\phi_0 = 0$. For the case study of the DVB-NGH MIMO rate-2 system, the SNR can be determined by maximizing the following expression for various phase shift ϕ and amplitude A factors as

$$\text{SNR} = \frac{\left\| h_1 + A_1 e^{j\phi_1} h_2 \right\|^2}{E\left\| n_1 \right\|^2 + E\left\| A_1 e^{j\phi_1} n_2 \right\|^2} = \frac{\left\| h_1 + A_1 e^{j\phi_1} h_2 \right\|^2}{\sigma^2 \left(1 + A_1^2\right)}, \tag{19}$$

where σ^2 is the noise power.

In addition, multiple interferences in the DVB-NGH MIMO rate-2 system can be expressed as

$$\begin{aligned} r_1 &= h_1 x + h_{I1} s_I + n_1, \\ r_2 &= A_1 e^{j\phi_1} \left(h_2 x + h_{I2} s_I + n_2 \right), \\ y^{(h)} &= r_1 + r_2 = x\left(h_1 + A_1 e^{j\phi_1} h_2 \right) + s_I \left(h_{I1} + A_1 e^{j\phi_1} h_{I2} \right) + n_1 + A_1 e^{j\phi_1} n_2, \end{aligned} \tag{20}$$

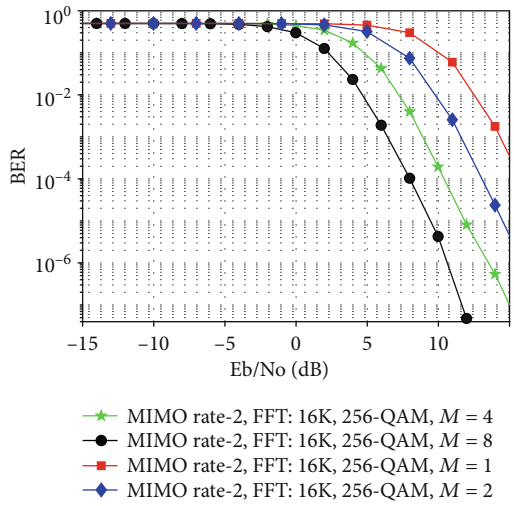

Figure 5: The BER performance against Eb/No for MIMO rate-2 using the modulation scheme of 256-QAM and the FFT size of 16 K for various transmitter antennas of $M = 1, 2, 4$, and 8.

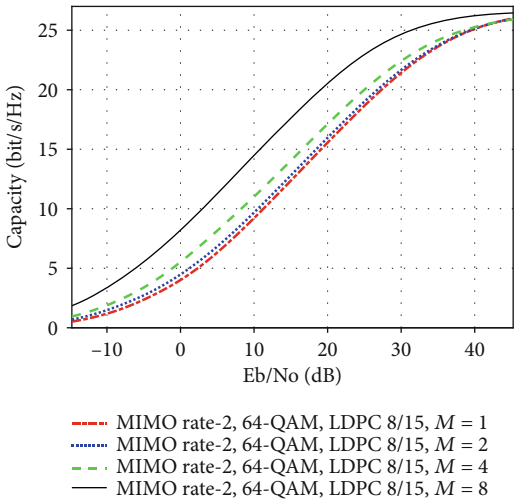

Figure 6: Capacity achieved by various transmitter antennas for a MIMO rate-2 mode with the modulation scheme of 64-QAM and the inner coding of LDPC 8/15.

where s_I represents the interference signal. For the case of DVB-NGH MIMO system using N transmitter and M receiver antennas, the received signal is represented as

$$r_k = \sum_{i=1}^{N} \left(A_k e^{j\phi_k} h_{ik} x + A_k e^{j\phi_k} h_{Ik} s_I + A_k e^{j\phi_k} n_k \right), \tag{21}$$

and the output of the analog beamformer is expressed as

$$y_k = \sum_{i=1}^{M} r_k. \tag{22}$$

The signal-to-interference-and-noise ratio (SINR) which corresponds to the signal strength parameter can be then determined for the DVB-NGH MIMO rate-2 system. The

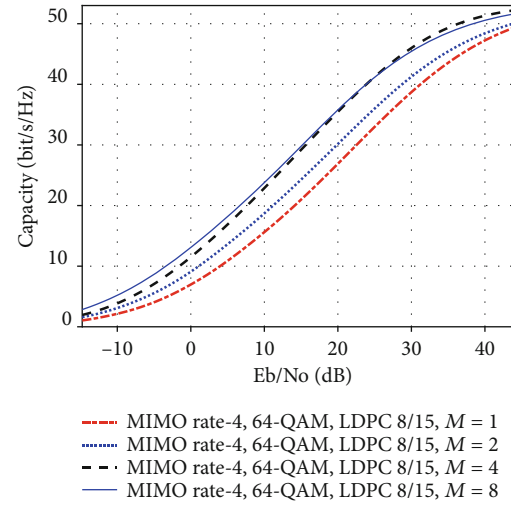

Figure 7: Capacity achieved by various transmitter antennas for a MIMO $N_s = 4$ mode with the modulation scheme of 64-QAM and the inner coding of LDPC 8/15.

SINR can be determined by maximizing the following expression for various phase shift ϕ and amplitude A factors as

$$\begin{aligned} \text{SINR} &= \frac{\left\| h_1 + A_1 e^{j\phi_1} h_2 \right\|^2}{E\|n_1\|^2 + E\left\| A_1 e^{j\phi_1} n_2 \right\|^2 + \left\| h_{I1} + A_1 e^{j\phi_1} h_{I2} \right\|^2} \\ &= \frac{\left\| h_1 + A_1 e^{j\phi_1} h_2 \right\|^2}{\sigma^2 \left(1 + A_1^2\right) + \left\| h_{I1} + A_1 e^{j\phi_1} h_{I2} \right\|^2}, \end{aligned} \tag{23}$$

where σ^2 is the noise power.

When the desired signal has $i = 1, \cdots, P$ multiple paths with different delays and the interfering signal has multiple paths $k - 1, \cdots, R$ with different delays, then the maximum SINR solution for the DVB-NGH MIMO rate-2 system in that case is given by

$$\text{SINR}_{\max} = \frac{\sum_{i=1}^{P} \left\| h_1 + A_1 e^{j\phi_1} h_2 \right\|^2}{\sigma^2 \left(1 + A_1^2\right) + \sum_{k=1}^{R} \left\| h_{I1} + A_1 e^{j\phi_1} h_{I2} \right\|^2}. \tag{24}$$

The corresponding achievable average capacity can be rewritten as [32]

$$C_H = \mathbb{E}_{\mathbf{H}}[\log_2(1 + \text{SINR}_{\max})]. \tag{25}$$

To reduce the computational complexity, numerous suboptimal MIMO receivers have been used such as the linear zero-forcing (ZF) and the minimum mean square error (MMSE) receivers [34]. The optimum receiver, i.e., the ML detector at the receiver, evaluates the squared Euclidean distance $D(x_1, x_2)$ and selects the coupe (x_1, x_2) minimizing this distance. The squared Euclidean distance can be expressed as

$$\begin{aligned} D(x_1, x_2) &= \|\mathbf{Y} - \mathbf{H}\mathbf{x}\|_F^2 = \|r_1 - h_{11}x_1 - h_{12}x_2\|^2 \\ &\quad + \|r_2 - h_{21}x_1 - h_{22}x_2\|^2, \end{aligned} \tag{26}$$

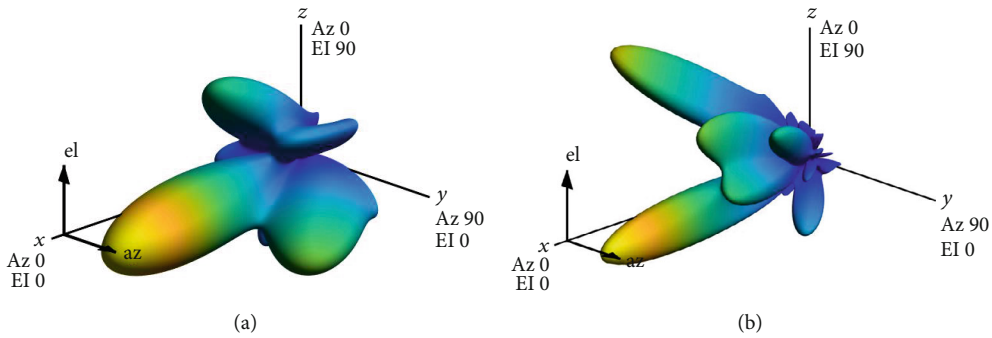

FIGURE 8: Beampattern of the proposed beamforming scheme: (a) $M_T = 8$ and $M_R = 2$ for the MIMO rate-2 mode; (b) $M_T = 16$ and $M_R = 4$ for the MIMO $N_s = 4$ mode.

where $\|.\|_F^2$ is the Frobenius norm and $\mathbf{Y}$ is the received noisy signal.

4. Simulation Results

In this section, we show the BER performance of the proposed system by means of the Monte Carlo simulation. The simulation estimates the capacity performance versus the signal-to-noise ratio and bit error rate versus Eb/No ratio. Table 2 shows two study cases for the performance evaluation of the proposed system. In the first case, the MIMO rate-2 for the FFT 8 K/16 K mode is performed using 64-QAM or 256-QAM modulation constellation schemes. In the second case, the MIMO rate-2 for the number of substreams of 2 and 4 over the 16 K FFT mode is performed using 64-QAM. Within each study case, we evaluate system parameters with various analog precoder configurations. The detailed simulation parameters are presented in Table 3. The simulations include inner LDPC codes with a word length size of 16200 bits (16 K) and the outer BCH.

Figure 4 shows the bit error rate (BER) performance versus Eb/No for the various M values of 1 and 2. We evaluate all combinations of constellation orders 64-QAM and 256-QAM with the FFT size of 8 K and 16 K. It is clearly noted that the system's performance significantly increases when the power gain increases. In addition, figures also show that increasing the FFT size severely improves the BER performance, especially at the power gain of 10 dB. However, for the case of $M = 4$, it is noted that the best system performance can be achieved at the power gain of approximately 7.5 dB for the case of MIMO rate-2, the FFT size of 16 using 64-QAM modulation scheme.

In Figure 5, we show the BER performance of the DVB-NGH system versus the Eb/No for MIMO rate-2 using the 256-QAM modulation scheme and the FFT size of 16 K for various transmitter antennas of $M = 1$, 2, 4, and 8. It is also seen that the BER decreases with the increase of Eb/No. In addition, the increase of the number of transmitter antennas significantly increases the DVB-NGH system performance. The power gain of approximately 5 dB is seen when increasing the number of transmitter antennas from 1 to 2, 2 to 4, and 4 to 8, at the target BER less than 10^{-3}.

Now, let us evaluate the proposed hybrid beamforming dual-polarized MIMO spatial multiplexing with the eSM-PH structure. Figures 6 and 7 present the system capacity achieved by the modulation scheme of 64-QAM, the inner coding of LDPC 8/5, and a frame error rate (FER) 1% after BCH. The analyzed schemes are MIMO rate-2 and MIMO with four RF chains ($N_s = 4$) with $M = 1, 2, 4, 8$ for performance comparison purposes. The channel model used for this case study is uncorrelated Rayleigh fading in which the impairment correlation factor between the antenna elements is 1%. The results illustrate a better performance with various M values. The beamforming gains achieved with LDPC code rate 8/15 at BER of 10^{-4} decoding increase with the number of elements at analog precoder, i.e., 3 dB ($M = 2$), 6 dB ($M = 4$), and 8.9 dB ($M = 8$).

Finally, Figure 8 shows the beampattern of the proposed hybrid beamformer with two RF chains ($N_s = 2$) and number of the antennas $M_T = 8$ and $M_R = 2$ (Figure 8(a)) and four RF chains ($N_s = 4$) $M_T = 16$ and $M_R = 4$ (Figure 8(b)). It can be seen from the proposed scheme that the optimized beamformer has dominant beams. This beampattern means that the data streams can be successfully transmitted through those beams.

5. Conclusions

In this paper, we developed a new beamforming scheme based on hybrid beamforming and dual-polarized MIMO spatial multiplexing for DVB-NGH systems. In the proposed approach, the beamforming scheme has maximized the channel capacity of the MIMO-based DVB-NGH systems. Simulation results showed that the proposed hybrid beamforming is efficient to achieve higher capacity than the existing dual-polarized MIMO spatial multiplexing for the DVB-NGH systems. The performance evaluation in terms of the bit error rate, the ergodic channel capacity, and the beampatterns showed that the proposed hybrid beamforming schemes using analog-digital beamforming and dual-polarized MIMO spatial multiplexing for the DVB-NGH system have dominant beams. Although some achievements have been achieved, some challenging problems remain to be solved, for example, physical size reduction. Therefore, in the future work, the hybrid beamforming configuration scheme could be optimized for the handheld receiver in DVB-NGH systems.

Data Availability

The data used to support the findings of this study are included within the article. Simulation experiments were carried out using MATLAB®. All data used to support the findings of this study are included within the article. The latter are available from the corresponding author upon request.

Conflicts of Interest

The authors declare that there is no conflict of interest regarding the publication of this paper.

Acknowledgments

This work is supported by Ministry of Science and Technology of Vietnam under Project No. NDT.32.ITA/17.

References

[1] D. Gómez-Barquero, Ed., *Next Generation Mobile Broadcasting*, CRC Press, 2013.

[2] G. Faria, J. A. Henriksson, E. Stare, and P. Talmola, "DVB-H: digital broadcast services to handheld devices," *Proceedings of the IEEE*, vol. 94, no. 1, pp. 194–209, 2006.

[3] M. R. Chari, F. Ling, A. Mantravadi et al., "FLO physical layer: an overview," *IEEE Transactions on Broadcasting*, vol. 53, no. 1, pp. 145–160, 2007.

[4] I. Andrikopoulos, N. Chuberre, M. Cohen et al., "An overview of digital video broadcasting via satellite services to handhelds (DVB-SH) technology," in *Handbook of Mobile Broadcasting: DVB-H, DMB, ISDB-T and MediaFLO*, CRC Press, 2008.

[5] DVB Document A160, *Digital video broadcasting (DVB); next generation broadcasting system to handheld, physical layer specification (DVB-NGH)*, 2012.

[6] L. Vangelista, N. Benvenuto, S. Tomasin et al., "Key technologies for next-generation terrestrial digital television standard DVB-T2," *IEEE Communications Magazine*, vol. 47, no. 10, pp. 146–153, 2009.

[7] I. Eizmendi, G. Prieto, G. Berjon-Eriz, I. Landa, and M. Velez, "Empirical DVB-T2 thresholds for fixed reception," *IEEE Transactions on Broadcasting*, vol. 59, no. 2, pp. 306–316, 2013.

[8] D. Gómez-Barquero, C. Douillard, P. Moss, and V. Mignone, "DVB-NGH: the next generation of digital broadcast services to handheld devices," *IEEE Transactions on Broadcasting*, vol. 60, no. 2, pp. 246–257, 2014.

[9] J. J. Giménez, E. Stare, S. Bergsmark, and D. Gomez-Barquero, "Advanced network planning for time frequency slicing (TFS) toward enhanced efficiency of the next-generation terrestrial broadcast networks," *IEEE Transactions on Broadcasting*, vol. 61, no. 2, pp. 309–322, 2015.

[10] H. Schwarz, D. Marpe, and T. Wiegand, "Overview of the scalable video coding extension of the H.264/AVC standard," *IEEE Transactions on Circuits and Systems for Video Technology*, vol. 17, no. 9, pp. 1103–1120, 2007.

[11] J. Lopez-Sanchez, J. Zollner, S. Atungsiri, E. Stare, and D. Gomez-Barquero, "Technical solutions for local service insertion in DVB-NGH single frequency networks," *IEEE Transactions on Broadcasting*, vol. 60, no. 2, pp. 293–301, 2014.

[12] Y. Zhang, C. Zhang, J. Cosmas et al., "Analysis of DVB-H network coverage with the application of transmit diversity," *IEEE Transactions on Broadcasting*, vol. 54, no. 3, pp. 568–577, 2008.

[13] H. Luo, Y. Zhang, L.-K. Huang, J. Cosmas, and A. Aggoun, "A closed-loop reciprocity calibration method for massive MIMO in terrestrial broadcasting systems," *IEEE Transactions on Broadcasting*, vol. 63, no. 1, pp. 11–19, 2017.

[14] L. Dai, Z. Wang, and Z. Yang, "Next-generation digital television terrestrial broadcasting systems: key technologies and research trends," *IEEE Communications Magazine*, vol. 50, no. 6, pp. 150–158, 2012.

[15] D. Vargas, Y. J. D. Kim, J. Bajcsy, D. Gomez-Barquero, and N. Cardona, "A MIMO-channel-precoding scheme for next generation terrestrial broadcast TV systems," *IEEE Transactions on Broadcasting*, vol. 61, no. 3, pp. 445–456, 2015.

[16] D. Vargas, D. Gozalvez, D. Gomez-Barquero, and N. Cardona, "MIMO for DVB-NGH, the next generation mobile TV broadcasting [accepted from open call]," *IEEE Communications Magazine*, vol. 51, no. 7, pp. 130–137, 2013.

[17] J. H. Seo, T. J. Jung, H. M. Kim, and D. S. Han, "Improved polarized 2x2 MIMO spatial multiplexing method for DVB-NGH system," *IEEE Transactions on Broadcasting*, vol. 61, no. 4, pp. 729–733, 2015.

[18] F. Sohrabi and W. Yu, "Hybrid digital and analog beamforming design for large-scale MIMO systems," in *2015 IEEE International Conference on Acoustics, Speech and Signal Processing (ICASSP)*, Brisbane, Australia, 2015.

[19] F. Sohrabi and W. Yu, "Hybrid digital and analog beamforming design for large-scale antenna arrays," *IEEE Journal of Selected Topics in Signal Processing*, vol. 10, no. 3, pp. 501–513, 2016.

[20] A. Alkhateeb, O. El Ayach, G. Leus, and R. Heath, "Channel estimation and hybrid precoding for millimeter wave cellular systems," *IEEE Journal of Selected Topics in Signal Processing*, vol. 8, no. 5, pp. 831–846, 2014.

[21] O. El Ayach, S. Rajagopal, S. Abu-Surra, Z. Pi, and R. Heath, "Spatially sparse precoding in millimeter wave MIMO systems," *IEEE Transactions on Wireless Communications*, vol. 13, no. 3, pp. 1499–1513, 2014.

[22] R. Magueta, D. Castanheira, A. Silva, R. Dinis, and A. Gameiro, "Hybrid multi-user equalizer for massive MIMO millimeter-wave dynamic subconnected architecture," *IEEE Access*, vol. 7, pp. 79017–79029, 2019.

[23] R. Magueta, D. Castanheira, P. Pedrosa, A. Silva, R. Dinis, and A. Gameiro, "Iterative analog–digital multi-user equalizer for wideband millimeter wave massive MIMO systems," *Sensors*, vol. 20, no. 2, p. 575, 2020.

[24] M. Hefnawi, "Hybrid beamforming for millimeter-wave heterogeneous networks," *Electronics*, vol. 8, no. 2, p. 133, 2019.

[25] E. G. Larsson, "Joint beamforming and broadcasting in massive MIMO," in *2015 IEEE 16th International Workshop on Signal Processing Advances in Wireless Communications (SPAWC)*, pp. 266–270, Stockholm, Sweden, 2015.

[26] I.-W. Kang, K. H. Suh, H. M. Kim et al., "Performance of MIMO bit division with polarized MIMO DVB-T2," in *Proceedings of International Conference on Systems and Electronic Engineering (ICSEE'2012)*, pp. 57–60, Phuket, Thailand, 2012.

[27] C. Douillard and C. A. Nour, "The bit interleaved coded modulation module for DVB-NGH: enhanced features for mobile

reception," in *2012 19th International Conference on Telecommunications (ICT)*, pp. 1–6, Jounieh, Lebanon, 2012.

[28] N. H. Trung, N. T. Anh, N. M. Duc, D. T. Binh, and L. T. Tan, "System theory based multiple beamforming," *Vietnam Journal of Science and Technology*, vol. 55, no. 5, p. 637, 2017.

[29] N. H. Trung and D. T. Binh, "Large-scale MIMO MC-CDMA system using combined multiple beamforming and spatial multiplexing," *Vietnam Journal of Science and Technology*, vol. 56, no. 1, pp. 102–112, 2018.

[30] F. Zheng, Y. Chen, B. Pang et al., "An efficient CSI feedback scheme for dual-polarized massive MIMO," *IEEE Access*, vol. 6, pp. 23420–23430, 2018.

[31] O. Alluhaibi, Q. Z. Ahmed, C. Pan, and H. Zhu, "Capacity maximisation for hybrid digital-to-analog beamforming mm-wave systems," in *2016 IEEE Global Communications Conference (GLOBECOM)*, Washington, DC, USA, 2016.

[32] E. Telatar, "Capacity of multi-antenna Gaussian channels," *European Transactions on Telecommunications*, vol. 10, no. 6, pp. 585–595, 1999.

[33] M. Abdelaziz, L. Anttila, A. Brihuega, F. Tufvesson, and M. Valkama, "Digital predistortion for hybrid MIMO transmitters," *IEEE Journal of Selected Topics in Signal Processing*, vol. 12, no. 3, pp. 445–454, 2018.

[34] X. Liu, Q. Zhang, W. Chen et al., "Beam-oriented digital predistortion for 5G massive MIMO hybrid beamforming transmitters," *IEEE Transactions on Microwave Theory and Techniques*, vol. 66, no. 7, pp. 3419–3432, 2018.